

OPEN QUANTUM SYSTEMS, ENTROPY AND CHAOS^a

HANS-THOMAS ELZE

*Universidade Federal do Rio de Janeiro, Instituto de Física
Caixa Postal 68.528, 21945-970 Rio de Janeiro, RJ, Brasil*

and

Physics Department, University of Arizona, Tucson, AZ 85721

Entropy generation in quantum systems is tied to the existence of a nonclassical environment (heat bath or other) with which the system interacts. The continuous ‘measuring’ of the open system by its environment induces decoherence of its wave function and entropy increase. Examples of nonrelativistic quantum Brownian motion and of interacting scalar fields illustrate these general concepts. It is shown that the Hartree-Fock approximation around the bare ($\hbar = 0$) classical limit can lead to spurious semiquantum chaos, which may affect the determination of entropy production and thermalization also in other cases.

1 Introduction

The related topics of environment induced quantum decoherence and the transition from quantum to classical mechanics have recently been investigated in widely varying contexts, ranging from problems of interpretation of quantum mechanics, of the measurement process in particular, to questions of how classical physical laws and the observed classical features of cosmology emerge in the underlying quantum universe, see e.g. Refs.^{1–5}. The central idea of the quantum decoherence approach is that the transition *quantum* \rightarrow *classical* can be understood as a dynamical effect within quantum mechanics itself, especially keeping \hbar nonzero as it is.

In this lecture I will explain some of these issues, in particular how *entropy generation* is intimately related to an *open quantum system*. Its identification, its properties, and the calculation of the time dependent entropy production present unresolved problems for strongly interacting systems, such as the high energy density matter formed during relativistic hadronic or nuclear collisions. Based on more technical details given in Refs.⁶, I will outline how the quantum decoherence approach can be applied here.

This is obviously related to the persistent issue of thermalization of strongly interacting matter, the assumption of which is one of the conceptual cornerstones guiding the ongoing search for the quark-gluon plasma (QGP), see Ref.⁷ and earlier “Quark Matter” proceedings. As reflected during this conference,

^aInvited talk presented at the 5th Rio de Janeiro International Workshop on Relativistic Aspects of Nuclear Physics, August 1997 — to be published in the proceedings, eds. T. Kodama et al. (World Scientific).

many theoretical attempts to pinpoint the most relevant QGP properties depart from the assumption of a thermalized high entropy density state of matter. However, at present we are still quite far from understanding how an initially ‘pure’ quantum state with zero entropy, e.g. two colliding nuclear wave packets, could evolve into the ‘mixed’ QGP state.

In order to fully appreciate the problem, we need a precise definition of the entropy, which preferably should allow us to extrapolate to the usual thermodynamical limit or Boltzmann’s entropy of statistical mechanics. Let us recall that the First Law of Thermodynamics relates infinitesimal changes of the internal energy U , the volume V , and the entropy S , given the pressure P and the temperature T of the system:

$$dU = -PdV + \delta Q = -PdV + TdS \quad . \quad (1)$$

Thus, the change of the internal energy is related to the work done by the system against the external pressure and to the heat δQ transfer or the entropy change, respectively. The Second Law of Thermodynamics rules that the entropy in a *closed* system cannot decrease:

$$\frac{dS(t)}{dt} \geq 0 \quad . \quad (2)$$

Furthermore, based on a statistical definition of the (N -particle) entropy,

$$S_B(t) \equiv -k_B \int \frac{d^{3N}x \, d^{3N}p}{(2\pi\hbar)^{3N}} f(x, p; t) \ln f(x, p; t) \quad , \quad (3)$$

employing a suitable phase-space distribution function, one is led to the interpretation due to Boltzmann that the entropy measures the observer’s *lack of information* about the system. It determines the number of possible realizations (microstates) of the system which conform with a given macrostate specified, for example, in terms of the above thermodynamical variables.

Evidently, in relativistic heavy-ion physics much use is made of such related thermodynamical notions as equilibration, thermal p_\perp -spectra, equation of state, phase transition, etc.

It is our aim here to get a quantum mechanical handle on the entropy. – As is well known, the Wigner function is what comes closest to a quantum mechanical distribution function replacing $f(x, p; t)$ ⁸; see Ref.⁹ for a review of earlier work on quark-gluon transport theory, i.e. the dynamics of QCD Wigner functions. For our present purposes it is more convenient to work with density matrices, which generally are related to Wigner functions by appropriate Fourier transforms. – In terms of the density operator $\hat{\rho}$ characterizing a (closed) quantum mechanical system, we will henceforth employ the

von Neumann definition of the entropy^{1,8}:

$$S(t) \equiv -\text{Tr } \hat{\rho}(t) \ln \hat{\rho}(t) = - \sum_n w_n \ln w_n \quad (4)$$

where the trace is over a complete set of states and w_n denotes the probability of such a state $|n\rangle$; from now on we employ units such that $\hbar = c = k_B = 1$, except when stated otherwise.

As we shall see in the next section, the von Neumann entropy has several desirable properties, but shows some surprising features as well. Most notably $S \equiv 0$ for closed systems. The latter result has led to some confusion in the past¹⁰, in particular it has been claimed that S , as defined here, is completely useless, if one wants to characterize the entropy production in high-energy physics. However, these objections are overcome by the decoherence approach and especially by realizing that in this case, like in most if not all physically interesting cases, the system is open indeed.

2 The von Neumann Entropy and the Need for Open Systems

In order to illustrate some important features of the entropy S , as defined in eq. (4), we evaluate it for two limiting cases, for a quantum system in a pure state and in the thermal equilibrium state, respectively. An elementary example for a two-state system is given in Ref.^{6(c)}.

If the system is in a *pure state* $|\Psi\rangle$, the density operator assumes the simple form $\hat{\rho} = |\Psi\rangle\langle\Psi|$. Correspondingly, the probability of finding the system in this state is $w_\Psi = 1$. Therefore, we obtain immediately:

$$S_\Psi = -1 \cdot \ln 1 = 0 \quad , \quad (5)$$

which can be interpreted that we know everything about the system that we possibly can.

Similarly one finds that if the system is in any one of N states with equal probability $1/N$, then the entropy equals $\ln N$, i.e. the maximum value, when we are completely ignorant about which state the system is in.

Let us consider one of the most important cases of an impure or *mixed state*, namely when the system is in thermal equilibrium. Then, the density operator is given by:

$$\hat{\rho} = Z^{-1} e^{-\beta \hat{H}} \quad , \quad Z \equiv \text{Tr } e^{-\beta \hat{H}} = \sum_n e^{-\beta E_n} \quad , \quad (6)$$

where Z is the partition function, \hat{H} is the Hamiltonian, and $\beta \equiv T^{-1}$ denotes the inverse temperature of the system. We find:

$$\begin{aligned} S(T) &= - \sum_n \frac{e^{-\beta E_n}}{Z} \ln \frac{e^{-\beta E_n}}{Z} = \ln Z - \text{Tr} \frac{e^{-\beta \hat{H}}}{Z} (-\beta \hat{H}) \\ &= \ln Z - Z^{-1} \beta \partial_\beta Z = \partial_T (T \ln Z) \equiv -\partial_T F , \end{aligned} \quad (7)$$

which relates the von Neumann entropy to the usual partial derivative of the free energy, which is familiar from thermodynamics.

The properties of the entropy which we have considered so far tie in with our knowledge of thermodynamics or classical statistical mechanics. However, a problem arises immediately, since the entropy S turns out to be a constant of motion. According to the Schrödinger equation the time evolution of wave functions is unitary, $|\Phi(t)\rangle = \exp(-i\hat{H}t)|\Phi(0)\rangle$, which implies:

$$S(t) = -\text{Tr} \left\{ e^{-i\hat{H}t} \hat{\rho}(0) e^{i\hat{H}t} \ln [e^{-i\hat{H}t} \hat{\rho}(0) e^{i\hat{H}t}] \right\} = S(0) , \quad (8)$$

using the cyclic property of the trace. In a closed system the entropy stays constant at the initial value.

More specifically, the unitary quantum mechanical time evolution prohibits a transition from a zero entropy pure initial state to a mixed nonzero entropy final state. However, it is well known how to overcome this impasse. Similarly as in classical statistical mechanics, where coarse graining in phase space allows to circumvent $df/dt = 0$ (Liouville flow) and hence $\dot{S}_B = 0$, cf. eq. (3), we have to give up the premise of unitary time evolution.

The decoherence approach is based on a separation of ‘all degrees of freedom’ into the observed degrees of freedom (*system*) and the ‘rest of the universe’ (*environment*)^{1,2,4}. The border between system and environment generally has to be open to the exchange of information and possibly to the exchange of energy, momentum, etc. Without interaction two isolated closed systems result. Then, the density operator $\hat{\rho}$ representing all degrees of freedom (d.o.f.) evolves unitarily and the corresponding entropy is a constant, as we have shown. However, the density operator $\hat{\rho}_S$ representing the system,

$$\hat{\rho}_S(t) = \text{Tr}_E \hat{\rho}(t) , \quad (9)$$

which is obtained by tracing over the environment degrees of freedom, evolves in a more complicated non-unitary way. Consequently, the entropy of the system $S_S(t)$, which is defined as the von Neumann entropy employing $\hat{\rho}_S(t)$, will change in time, as we shall see.

The non-unitary evolution of the system density matrix is accompanied by *environment induced decoherence*, i.e. typically its off-diagonal elements which encode the quantum mechanical interference effects decay with a characteristic decay constant τ_D . Correspondingly, the eigenvalues of $\hat{\rho}_S$ change and the diagonal matrix elements become probabilities characterizing the resulting mixed state. If there is thermalization,

$$\rho_S^{nn}(t) \xrightarrow{\tau_{th}} \frac{e^{-\beta E_n}}{Z} , \quad (10)$$

i.e. the diagonal matrix elements become the usual Boltzmann weights, cf. eqs. (6), (7). Most interestingly, the decoherence time τ_D is found to be several ten orders of magnitude smaller than the thermalization time τ_{th} for models of macroscopic bodies interacting with their environment (cosmic background radiation, atmospheric gas particles, etc.)¹¹. This explains the classical behavior of most of what we observe in daily life¹. Cases of quantum decoherence and ‘revival’ of the off-diagonal matrix elements are also known and experimentally observed in cavity quantum electrodynamics.

For microscopic systems, generally, the situation is more intricate and depends sensitively on the interactions and the separation into system and environment d.o.f., in particular for more complex systems than a single particle or one d.o.f. interacting with an environment¹¹. If we find $\tau_D \ll \tau_{th}$, then the possibility arises of creating a system with high entropy which is not at all thermalized. We would like to know precisely how these time scales compare in high-energy collisions of hadrons or nuclei and, of course, to what extent these systems thermalize.

Next, we present the useful theorem that the entropy generated in a system exactly equals the entropy generated in its environment due to the *mutual* decoherence process,

$$S_S(t) = -\text{Tr } \hat{\rho}_S(t) \ln \hat{\rho}_S(t) = -\text{Tr } \hat{\rho}_E(t) \ln \hat{\rho}_E(t) = S_E(t) , \quad (11)$$

with $\hat{\rho}_E$ calculated from $\hat{\rho}$ by tracing over the system d.o.f. analogously to $\hat{\rho}_S$, eq. (9). This result follows from the Schmidt decomposition of the density matrices^{6(a)}, which is for matrices (e.g. in Hilbert space) what the Schmidt orthogonalization procedure is for vectors.

This leads us to the question, whether the hard as well as the large number of soft *photons* generated by bremsstrahlung from quarks during the initial hard scattering and stopping phase of a hadronic collision yield an important decoherence effect. This would imply that a major part of the entropy observed in the final hadronic states of the reaction is already generated during its

initiation. A simple counting argument based on the ratio of effective photon and QGP d.o.f., i.e. their entropy ratio in thermal equilibrium,

$$\frac{N_\gamma}{N_{QGP}} = \frac{2\tilde{\sigma}VT^3}{37\tilde{\sigma}VT^3} , \quad (12)$$

seems to indicate that only about 5% (or less) of the entropy can be generated in this way. Note, however, the strong temperature dependence of the absolute numbers. Even if it does not maximize the entropy, as a thermal distribution does, a nonequilibrium distribution generated by bremsstrahlung processes which effectively corresponds to a higher photon ‘temperature’ may lead to a sizeable correction of the above estimate. The discussion following eq. (5) explains that generally a flat distribution contains less information/more entropy than a steep one and that the size of the available phase space matters (‘ $\ln N$ ’). A dynamical calculation generalizing results presented in the following Sections 3 and 4 is presently carried out.

In the example just considered the separation between system and environment d.o.f. is based on the fact that the strongly interacting system of quarks and gluons is essentially bound for, say, 10 fm/c until ‘freeze-out’, whereas the nonequilibrium environment photons are generated particularly during the first 0.1 ... 0.5 fm/c and essentially free to leave. Thus the ‘rest of the universe’ or *environment* is open to interpretation and has to be determined according to the physical circumstances.

3 A Nonrelativistic Quark in Brownian Motion

The purpose of this section is to demonstrate how the general concepts of environment induced decoherence and entropy generation in an open quantum system work in practice. The example can be understood as a nonrelativistic (heavy) quark moving and interacting with its own gluonic environment field, the properties of which can only be modelled at present.

We start with a model Hamiltonian describing the bilinear translation invariant interaction between a nonrelativistic particle (*system*) and an infinite set of harmonic oscillators (*environment*):

$$H = \frac{p^2}{2M} + \sum_{\omega_n \leq \Omega} \left\{ \frac{P_n^2}{2m_n} + \frac{1}{2}m_n\omega_n^2(X_n - x)^2 \right\} , \quad (13)$$

where Ω presents a high-frequency cut-off (such as Debye frequency and inverse classical electron radius in similar models related to the polaron and electron, respectively); we may think of the QCD scale parameter $\Lambda_{QCD} \approx 200 \text{ MeV}$.

This type of model associated with the names of Feynman and Vernon or Caldeira and Leggett has been extensively studied in the field of quantum Brownian motion¹², developing further the original Feynman-Vernon influence functional technique.

As it turns out, the physics described by the model of eq. (13) is completely determined by the spectral density distribution of the environment:

$$I(\omega) \equiv \frac{1}{2} \sum_{\omega_n \leq \Omega} m_n \omega_n^3 \delta(\omega - \omega_n) , \quad (14)$$

and the related noise and dissipation kernels¹². – For the polaron and electron cases one obtains $I(\omega) \propto \omega^3$ for $\omega \rightarrow 0$, which lead to the well known mass renormalization for $t \rightarrow \infty$, whereas for an ‘Ohmic’ environment one chooses $I(\omega) \propto \omega$, leading to a dissipative force proportional to the velocity of the Brownian particle.

Unfortunately, in the QCD case we do not know how to calculate the spectral density distribution. Classically QCD is a nonintegrable theory, which implies that such a decoupled oscillator representation of the dynamics does *not* exist¹³. Therefore, it seems unlikely that standard perturbation theory, which is based on the \hbar -(loop-)expansion around the naive classical limit, can provide reliable results in this context.

Keeping this limitation in mind, I considered this model in the *strong-coupling limit* for $t \ll \Omega^{-1}$ at $T = 0$, where only certain moments of $I(\omega)$ enter the calculation and can be chosen as parameters of the model. Presently the spectral density is much larger in the infrared than in the polaron/electron case. Technical details of the calculation of the reduced density matrix propagator in the environment corresponding to eq. (13) can be found in Ref.⁶(a). Also longer time scales may be interesting to study.

Here we want to discuss only the very initial influence of the environment. Choosing $I(\omega) \equiv g\Omega^3 F(\omega/\Omega)\Theta(\Omega - \omega)$, with an undetermined shape function F and dimensionless coupling constant g , we have $g_0 \equiv g \int_0^1 dx x^{-1} F(x)$. Then, the following parameter and dimensionless time variable, respectively, are needed:

$$\alpha \equiv \frac{1}{2g_0} \frac{\Omega}{M} (w_0 \Omega)^{-4} , \quad t_+ \equiv \Omega t (2g_0 \frac{\Omega}{M})^{1/2} , \quad (15)$$

where w_0 denotes the initial ($t = 0$) width of a Gaussian wave packet representing a particle moving with the velocity $v_0 = \langle p \rangle_0 / M$ initially.

In Fig. 2 a) we observe the dissipative ‘friction’ effect of the environment. In the present approximation we obtain a universal curve showing the deceleration of the particle in terms of the time dependent velocity (divided by v_0) as a function of t_+ . For $g = 0$, of course, $v(t_+) = v_0$. Secondly, as shown

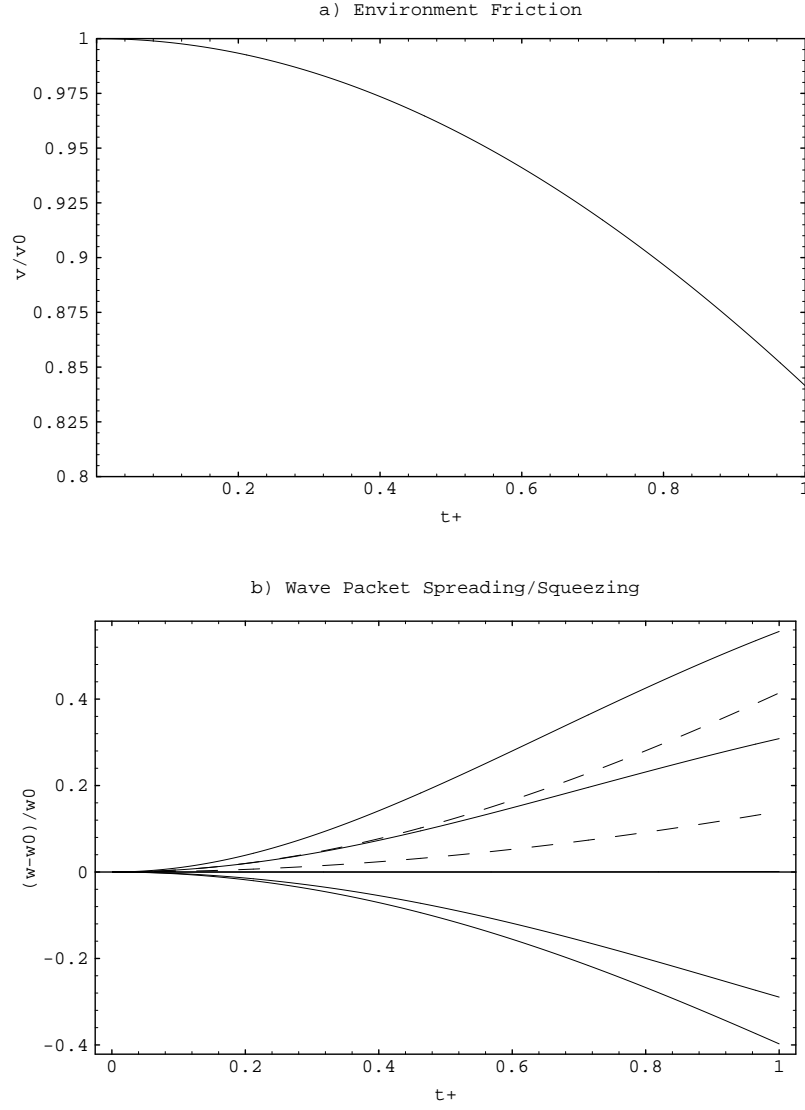


Figure 1: Environment effects in nonrelativistic quantum Brownian motion. a) The center of a Gaussian wave packet slows down. b) The width of the wave packet ($\alpha = 3.0, 2.0, 1.0, 0.3, 0.1$, full lines, top to bottom) expands more rapidly or may be squeezed as compared to the usual case ($\alpha = 1.0, 0.3$, upper and lower dashed curve, respectively). See main text for details.

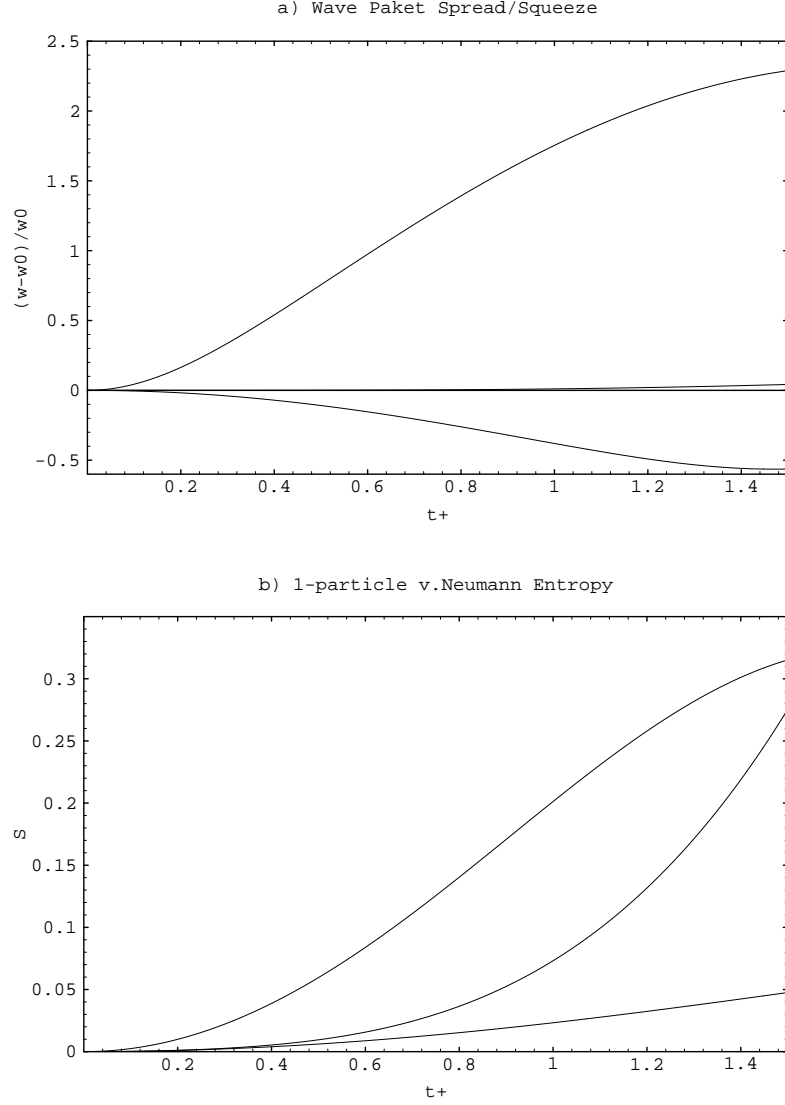


Figure 2: (a) Similar as Fig. 2 b), however, more extreme initial widths are considered – small, medium, and large wave packets (top to bottom), respectively. (b) The corresponding single particle entropy for a large, small, and medium size wave packet (top to bottom). See main text for details.

in Fig. 2 b), we find some surprising effects which the environment can have on the width of the wavepacket. There, the relative change of the width as a function of t_+ is represented: the wave packet spreads faster ($\alpha > 1$) than a corresponding free ($g = 0$) quantum mechanical wave packet, the width remains constant ($\alpha = 1$), or it even gets squeezed ($\alpha < 1$), depending on the parameter α . The dashed curves show the spreading for $g = 0$; they do not coincide because of the rescaled time axis. If the other physical model parameters were fixed, this result clearly shows that the particular coordinate-coordinate coupling between the particle and its environment, which we have chosen in eq. (13), is sensitive to the size of the particles' wave packet: sufficiently small packets spread faster than usual, sufficiently large ones get squeezed.

This is illustrated once more for some more extreme cases in Fig. 3 a), where the three curves (top to bottom) correspond to an initially small ($w_0\Omega \ll 1$), medium size ($w_0\Omega \approx 1$), and large ($w_0\Omega \gg 1$) wave packet, respectively. For these three cases we show in Fig. 3 b) the corresponding entropy, i.e. the entropy evaluated with the help of the time dependent density matrix of the nonrelativistic particle. In this figure the curves correspond to an initially large (top), small (middle), and medium size (bottom) wave packet, respectively. We do not attribute too much importance to the sizeable entropy which can be reached in very short time, e.g. $0.1 \text{ fm}/c$, since the numbers depend on the model parameters; we recall, however, the ultrarelativistic/high- T limit with 4 units of entropy per particle. – Actually represented here is the simpler *linear entropy*, $S_{lin} \equiv \text{Tr}[\hat{\rho} - \hat{\rho}^2]$, which provides a lower bound for the von Neumann entropy^{6(a)}. The linear and von Neumann entropies coincide in the zero and maximal entropy limits. – It is remarkable that medium size wave packets, the width of which is least affected by the environment, also generate the lowest entropy increase. They essentially behave like a *classical* particle.

Furthermore, coherent superpositions of such states decohere most quickly and show the strongest entropy generation^{6(a)}. These properties taken together qualify the Gaussian wave packets as approximate *pointer states* of the present model, similarly to the simple model studied in Ref.¹⁴. Pointer states show the behavior of a classical pointer^{1,2,3}: coherent superpositions of such states decohere very rapidly into mixed states, which are observed as various pointer positions with certain probabilities in a (macroscopic) experiment.

4 Interacting Scalar Fields

In this section we study two interacting scalar quantum fields, representing the *system* ('1') and *environment* ('2'), respectively. We want to describe their dynamics as well as the entropy generated in the system. We sketch this first

step in generalizing the Brownian motion example of Section 3 towards more realistic cases related to high-energy collisions, while the technical details may be found in Refs.⁶.

Let the classical action of this model be given as:

$$S \equiv \int d^4x \{L_1 + L_{12} + L_2\} \quad , \quad (16)$$

with the interaction potential $L_{12} = -V(\Phi_1, \Phi_2)$, and the Lagrangians:

$$L_j \equiv \frac{1}{2} \partial_\mu \Phi_j \partial^\mu \Phi_j - v_j(\Phi_j) \quad , \quad v(\Phi) \equiv -\frac{1}{2} \mu^2 \Phi^2 + \frac{1}{4!} \lambda \Phi^4 \quad . \quad (17)$$

Consider the separation into system and environment as originating from splitting a single scalar field, $\Phi \equiv \Phi_1 + \Phi_2$, according to some ‘coarse graining prescription’ to be discussed shortly. Then, the interaction potential is:

$$V(\Phi_1, \Phi_2) = -\mu^2 \Phi_1 \Phi_2 - \partial_\mu \Phi_1 \partial^\mu \Phi_2 + \frac{1}{4!} \lambda \Phi_1 \Phi_2 [4\Phi_1^2 + 6\Phi_1 \Phi_2 + 4\Phi_2^2] \quad . \quad (18)$$

We see that the bilinear coupling studied in most quantum Brownian motion models appears naturally here among other terms. Presently we will keep only this first term for simplicity, while results for a general quartic $V(\Phi_1, \Phi_2)$ are derived in Ref.^{6(a)}. – Now, various interpretations of the fields Φ_1, Φ_2 are possible:

- Coordinate space: Φ_1 and Φ_2 represent the same field, however, with support either inside the system or in the environment, respectively; $V(\Phi_1, \Phi_2)$ presents a contact interaction at the surface. Models of this type have been studied for the geometric entanglement entropy generated by event horizons (black holes), see e.g. Refs.¹⁵.
- Momentum space: Φ_1 and Φ_2 represent the long- and short-wavelength components of the same field. This has been of much interest in cosmology in the context of inflationary models; Ref.¹⁶ is a recent example, from which other references can be traced.

Strongly interacting matter naturally leads to a separation of d.o.f. In a finite size QGP droplet, with radius R on the order of a few fm, quark-gluon modes with wavelengths much larger than R are suppressed due to confinement and form an environment of virtual fluctuations together with composite meson (baryon) fields in the nonperturbative vacuum. Its properties, as with the case discussed in Section 3, cannot be calculated at present, but presumably play a crucial role in multiparticle production processes and the associated entropy generation. Finally, we mentioned before the bremsstrahlung photon environment which contributes to the decoherence of the charged quark system.

In the following we assume Φ_1 and Φ_2 to be two physically distinct fields.

4.1 Variational Approach to Time Evolution in Field Theory

We now turn to the dynamics of the coupled fields of our model defined in eqs. (16)–(18). The standard approach is motivated by perturbation theory, i.e. the usual \hbar -(loop-)expansion, and based on the Schwinger-Keldysh formalism. In order to resum the large class of (iterated bubble) diagrams corresponding to the time dependent Hartree-Fock approximation (TDHF), it is much more efficient to employ Dirac's time dependent variational principle.

The starting point is the *functional Schrödinger equation* describing the full dynamics of a generic field φ in the Schrödinger picture¹⁷:

$$i\partial_t \Psi[\varphi; t] = H[\hat{\pi}, \varphi] \Psi[\varphi; t] \equiv \int d^d x \left\{ -\frac{1}{2} \frac{\delta^2}{\delta \varphi^2} + \frac{1}{2} (\nabla \varphi)^2 + \mathcal{V}(\varphi) \right\} \Psi[\varphi; t] , \quad (19)$$

where $\Psi[\varphi; t] \equiv \langle \varphi | \Psi(t) \rangle$ denotes the wave functional in the φ -representation, which corresponds to a wave function $\psi(x, t) \equiv \langle x | \psi(t) \rangle$ for a one-dimensional quantum mechanical system, and $\hat{\pi} = -i\delta/\delta\varphi$ represents the canonical momentum operator conjugate to the field ('coordinate') φ . The dynamics is determined by the Hamiltonian H . In this context the completeness and inner product relation, respectively, involve functional integrals instead of ordinary ones (orthogonality needs a δ -functional), for example:

$$\langle \Psi_1(t) | \Psi_2(t) \rangle \equiv \int \mathcal{D}\varphi \langle \Psi_1(t) | \varphi \rangle \langle \varphi | \Psi_2(t) \rangle = \int \mathcal{D}\varphi \Psi_1^*[\varphi; t] \Psi_2[\varphi; t] , \quad (20)$$

with details to be found in Ref.^{6(a)}.

Then, we may state the *variational principle*:

$$\frac{\delta \Gamma[\Psi]}{\delta \Psi} = 0 , \quad \text{for all } \Psi \text{ with } \langle \Psi(t) | \Psi(t) \rangle = 1 , \quad (21)$$

$$\text{where } \Gamma[\Psi] \equiv \int dt \langle \Psi(t) | [i\partial_t - H] | \Psi(t) \rangle , \quad (22)$$

i.e. requiring the effective action Γ defined in eq. (22) to be stationary against arbitrary variations of the normalized wave functional Ψ , which vanish at $t \rightarrow \pm\infty$, is equivalent to the exact functional Schrödinger equation, eq. (19) above. With the variational principle in hand, one can solve the time evolution problem approximately by choosing a suitably parametrized trial wave functional. We remark that the effective action is real by construction.

We work with the most general Gaussian trial wave functionals. For a generic field φ it is defined by:

$$\Psi_G[\varphi; t] \equiv N(t) \exp\{ -[\varphi - \bar{\varphi}(t)] \left[\frac{1}{4} G^{-1}(t) - i\Sigma(t) \right] [\varphi - \bar{\varphi}(t)] + i\bar{\pi}(t) [\varphi - \bar{\varphi}(t)] \} , \quad (23)$$

where henceforth we do not explicitly write the integrations over spatial variables. For example,

$$\begin{aligned}\varphi G^{-1}(t)\bar{\varphi}(t) &\equiv \int d^d x d^d y \varphi(x) G^{-1}(x, y, t) \bar{\varphi}(y, t) , \\ \bar{\pi}(t)\varphi &\equiv \int d^d x \bar{\pi}(x, t) \varphi(x) , \quad \text{tr } \Sigma(t) \equiv \int d^d x \Sigma(x, x, t) .\end{aligned}\quad (24)$$

The normalization factor N (for symmetric and positive-definite G) is:

$$1 = \int \mathcal{D}\varphi \Psi_G^*[\varphi; t] \Psi_G[\varphi; t] \longrightarrow N(t) = (\mathcal{N} \det G(t))^{-1/4} , \quad (25)$$

cf. eq. (20) (\mathcal{N} is an infinite constant which we omit henceforth).

The meaning of the variational parameter functions $\bar{\varphi}$, $\bar{\pi}$, G , and Σ is discussed in Ref.^{6(a)}. The choice of Gaussian trial wave functionals is dictated by the need to evaluate functional integrals, in order to calculate the effective action Γ , eq. (22). The equivalence of this Hartree-Fock effective action with the Cornwall-Jackiw-Tomboulis generating functional for two-particle irreducible graphs was demonstrated in Ref.¹⁸ for energy eigenstates of the field. Variation of Γ w.r.t. to the parameter functions will give the dynamical equations, cf. Section 4.3 below, representing the field theory in terms of coupled equations for the one- and two-point Wightman functions.

We proceed with the ansatz for the two-field wave functional:

$$\begin{aligned}\Psi_{12}[\Phi_1, \Phi_2; t] &\equiv N_{12}(t) \Psi_{G_1}[\Phi_1; t] \Psi_{G_2}[\Phi_2; t] \\ &\cdot \exp \left\{ -\frac{1}{2} [\Phi_1 - \bar{\Phi}_1(t)] [G_{12}(t) - i\Sigma_{12}(t)] [\Phi_2 - \bar{\Phi}_2(t)] \right\} ,\end{aligned}\quad (26)$$

with the normalized Gaussians on the r.h.s. as defined in eq. (23), all terms carrying suitable indices for the field they belong to, and where N_{12} denotes an additional normalization factor. The latter is necessary, since we included an essential exponential describing the *two-point correlations* between the system and the environment fields. We obtain:

$$N_{12}(t) = (\det\{1 - G_1(t)G_{12}(t)G_2(t)G_{12}(t)\})^{1/4} , \quad (27)$$

similarly as in eq. (25).

Employing eq. (27), the calculation of the two-field effective action Γ is straightforward, even if tedious. We present here only the result for the simplest bilinear interaction, $V(\Phi_1, \Phi_2) \equiv -\mu^2 \Phi_1 \Phi_2$, while the case of a general

quartic interaction is studied in Ref.^{6(a)}:

$$\begin{aligned}
\Gamma[\Psi_{12}] = & \int dt \left\{ \sum_{j=1,2} \left\{ \bar{\Pi}_j \dot{\bar{\Phi}}_j - \frac{1}{2} \bar{\Pi}_j^2 - \frac{1}{2} (\nabla \bar{\Phi}_j)^2 - v_j(\bar{\Phi}_j) + \frac{1}{2} \mu^2 \bar{\Phi}_1 \bar{\Phi}_2 \right. \right. \\
& + \hbar \operatorname{tr} [\Sigma_j \dot{\bar{G}}_j - 2 \tilde{\Sigma}_j^2 \bar{G}_j - \frac{1}{8} G_j^{-1} [A + B] + \frac{1}{2} \nabla^2 \bar{G}_j] \\
& - \frac{\hbar}{2!} \langle v_j^{(2)} \rangle \operatorname{tr} \bar{G}_j - \frac{\hbar^2}{V_d} \frac{3}{4!} v_j^{(4)} (\operatorname{tr} \bar{G}_j)^2 \left. \right\} \\
& + \frac{\hbar}{2} \operatorname{tr} [\dot{\Sigma}_{12} \bar{G}_1 \bar{G}_2 \bar{G}_{12}] - \hbar \mu^2 \operatorname{tr} [\bar{G}_1 \bar{G}_2 \bar{G}_{12}] \left. \right\} , \quad (28)
\end{aligned}$$

with $v_j^{(n)} \equiv d^n v_j(\bar{\Phi}_j)/d\bar{\Phi}_j^n$, $\langle f \rangle \equiv \int d^d x f(x)/V_d$, and $V_d \equiv \int d^d x$. We also use the abbreviations $\bar{G}_{12} \equiv G_{12}[A - B]$, $\bar{G}_j \equiv [A - B]^{-1} G_j$, and ∇^2 acts on either one of the two formal spatial coordinates of \bar{G}_j ; furthermore, $\tilde{\Sigma}_1 \equiv \Sigma_1 - \frac{1}{4} G_2 G_{12} \Sigma_{12}$, and $\tilde{\Sigma}_2$ follows by $1 \leftrightarrow 2$; finally, $A - B \equiv 1 - G_1 G_2 G_{12}^2$ and $A + B \equiv 1 + G_1 G_2 \Sigma_{12}^2$. We recall that ‘products’ of two-point functions involve integrations over intermediate coordinates, which we suppressed as before. The two-point functions are assumed to be translation invariant (bulk matter).

Even for the simple bilinear interaction the effective action is quite complicated due to the full Hartree-Fock approximation for the system and environment fields. Note the $O(\hbar)$ and $O(\hbar^2)$ quantum corrections to the classical action, which appears in the first line of eq. (28). We observe that the dressing of the two-point functions G_1, G_2 by a geometric series of terms involving themselves and G_{12} disappears, as soon as the latter correlation function vanishes. The field equations resulting from the variations of the effective action are equally involved. In Section 4.3 we present a simplified version of them and some intriguing numerical results concerning the zero-dimensional limit, i.e. the quantum mechanical Hartree-Fock approximation.

4.2 The Entropy Functional

Knowing formally the wave functional of the system (Φ_1) coupled to the environment (Φ_2), we presently evaluate the von Neumann entropy of the system in terms of the two-point functions of the previous section and according to the outline in Section 2.

First of all, the system density functional is obtained from the total density

functional (matrix) by tracing over the environment d.o.f., cf. eq. (9):

$$\rho_S[\Phi_1, \Phi'_1; t] = \int \mathcal{D}\Phi_2 \langle |\hat{\rho}(t)| \Phi'_1, \Phi_2 \rangle = \int \mathcal{D}\Phi_2 \Psi_{12}^*[\Phi'_1, \Phi_2; t] \Psi_{12}[\Phi_1, \Phi_2; t] , \quad (29)$$

which is a Gaussian integral again. We obtain:

$$\rho_S[\Phi_1, \Phi'_1; t] = \tilde{\Psi}_{G_1}^*[\Phi'_1; t] \tilde{\Psi}_{G_1}[\Phi_1; t] \exp \{ Y_1^*[\Phi'_1; t] G_2(t) Y_1[\Phi_1; t] \} , \quad (30)$$

with:

$$Y_1[\Phi; t] \equiv \frac{1}{2} [\Phi - \bar{\Phi}_1] [G_{12}(t) - i\Sigma_{12}(t)] , \quad (31)$$

and where the effective Gaussian $\tilde{\Psi}_{G_1}$ here is defined as before, cf. eqs. (23) and (27), however, with the replacements:

$$\begin{aligned} N_1(t) &\longrightarrow \tilde{N}_1(t) \equiv N_1(t) N_{12}(t) , \\ G_1^{-1}(t) &\longrightarrow \tilde{G}_1^{-1}(t) \equiv G_1^{-1}(t) A(t) , \\ \Sigma_1(t) &\longrightarrow \tilde{\Sigma}_1(t) , \end{aligned} \quad (32)$$

with A and $\tilde{\Sigma}_1$ as introduced after eq. (28). Note that the result of eq. (31) has the typical form of a modified pure state density matrix times an exponential influence functional; both modifications vanish in the limit of vanishing correlations between system and environment.

In order to evaluate the entropy, i.e. $-\text{Tr} \rho_S \ln \rho_S$, we need to diagonalize the density matrix, such that its eigenvalues are accessible. This calculation was performed by functional means in Ref.^{6(b)}. The result can be represented in the form:

$$S_S(t) = - \int \frac{d^d k}{(2\pi)^d} \left\{ \ln(1 - Y_k) + \frac{Y_k}{1 - Y_k} \ln Y_k \right\} , \quad (33)$$

where X_k denotes the d-dimensional Fourier transform of $X(x)$, and we find:

$$Y_k = \frac{B_k}{A_k + (A_k^2 - B_k^2)^{1/2}} \quad (34)$$

$$\approx \kappa [G_1 G_2 (G_{12}^2 + \Sigma_{12}^2)]_k , \quad (35)$$

in terms of A, B as before, and where the constant κ is $1/4$ ($1/2$) in the small (large) entropy limit. We employed here that the products of translation invariant two-point functions involving integrations over intermediate coordinates become convolutions, which factorize after Fourier transformation. The

result in eq. (33) represents a sum of oscillator like terms, which could have been expected, cf. the first of Refs.¹⁵.

Several remarks are in order here:

- The results obtained are formally independent of the dynamics, which only enters through the actual time dependence of the two-point functions (the ‘mean fields’ $\bar{\Phi}_j, \bar{\Pi}_j$ do not contribute); however, their generality is restricted by the underlying ansatz of a Gaussian wave functional (TDHF), eq. (27).
- For *vanishing correlations* between system and environment (independent subsystems), $G_{12} = \Sigma_{12} = 0$, we obtain $S_S(t) = 0$.
- For small widths of the Gaussians, G_1 or G_2 small, the entropy is small. In this case the system or the environment follows a *quasi-classical trajectory* in ‘coordinate’ (field) space; the widths cannot be squeezed to zero because of the uncertainty principle, which is incorporated TDHF.

Employing the entropy, eq. (34), we define a dynamical time scale:

$$\tau_{(D, equ)}^{-1} \equiv \frac{d}{dt} \ln S_S(t) \approx \left(\frac{\int \dot{Y}_k \ln Y_k}{\int Y_k \ln Y_k}, -\frac{\int \dot{Y}_k / (1 - Y_k)}{\int \ln(1 - Y_k)} \right), \quad (36)$$

which determines the decoherence time τ_D and the equilibration time τ_{equ} in the limits of small and large entropies, respectively, as indicated.

The calculation of Ref.^{6(b)} yields as a side product the most probable eigenstate of the system density matrix, i.e. the *field pointer state* with the largest probability and the smallest (field) kinetic energy. It is a coherent state, i.e. Gaussian wave functional centered around the classical field configuration $\bar{\Phi}_1(x, t)$ with momentum $\bar{\Pi}_1$ and effective real width:

$$G_{eff} = \frac{4G_1}{1 - G_1 G_2 (G_{12}^2 - \Sigma_{12}^2) - (G_1 G_2 G_{12} \Sigma_{12})^2}, \quad (37)$$

to be compared with the bare width $4G_1$, in the absence of correlations. The special role of coherent states as pointer states of the electromagnetic field has also be found more recently in Ref.¹⁹, in a model of a dielectric medium.

4.3 Equations of Motion and Semiquantum Chaos

In order to illustrate the dynamical content of the effective action derived in Section 4.1, we consider simplified versions of the resulting equations of motion in this section, in particular also the case without environment. The full set

of equations for arbitrary quartic interactions within and between system and environment can be found in Ref.⁶(a).

Presently, we make the additional assumptions: i) We study only the infrared limit, i.e. quantum mechanics of spatially homogeneous coupled fields Φ_1, Φ_2 . ii) We neglect mean fields in the environment, $\bar{\Phi}_2, \bar{\Pi}_2 \approx 0$, and consider the case of small correlations G_{12}, Σ_{12} between system and environment.

Varying the effective action, eq. (28), and applying the above assumptions, we find the set of coupled nonlinear (first order) equations of motion :

$$\frac{\delta\Gamma}{\delta\bar{\Pi}_1} = 0 \implies \partial_t \bar{\Phi}_1 = \bar{\Pi}_1, \quad (38)$$

$$\frac{\delta\Gamma}{\delta\bar{\Phi}_1} = 0 \implies \partial_t \bar{\Pi}_1 = -v_1^{(1)} - \frac{\hbar}{2} v_1^{(3)} G_1, \quad (39)$$

$$\frac{\delta\Gamma}{\delta\Sigma_j} = 0 \implies \partial_t G_j = 4\Sigma_j G_j, \quad (40)$$

$$\frac{\delta\Gamma}{\delta\Sigma_{12}} = 0 \implies \partial_t G_{12} = -2(\Sigma_1 + \Sigma_2)G_{12} - \frac{1}{2}(G_1^{-1} + G_2^{-1})\Sigma_{12}, \quad (41)$$

Furthermore ($j' \neq j, j = 1, 2$):

$$\frac{\delta\Gamma}{\delta G_j} = 0 \implies \partial_t \Sigma_j = -2\Sigma_j^2 + \frac{1}{8}G_j^{-2} - \frac{1}{2}v_j^{(2)} - \frac{\hbar}{4}v_j^{(4)}G_j - \mu^2 G_{j'}G_{12}, \quad (42)$$

$$\frac{\delta\Gamma}{\delta G_{12}} = 0 \implies \partial_t \Sigma_{12} = -2(\Sigma_1 + \Sigma_2)\Sigma_{12} + \frac{1}{2}(G_1^{-1} + G_2^{-1})\Sigma_{12} + 2\mu^2, \quad (43)$$

where all quantities are simply functions of time; we combined the resulting equations in such a way that time derivatives on the r.h.s. were eliminated. Note that the terms $\propto \mu^2$ are due to the system-environment coupling.

Several features of eqs. (38)–(43) appear to be of a rather general nature. First of all, the ‘momenta’ $\bar{\Pi}_1, \Sigma_j$ can be easily eliminated. The resulting second order equations are of the (inhomogeneous) anharmonic oscillator type. They potentially become unstable due to a dynamical ‘negative mass squared’ term; in this case the effective potential corresponding to Γ has a complicated structure allowing for tunneling processes²⁰.

Furthermore, the coupled linear eqs. (41), (43) can be integrated formally. We consider here only the solution of one of them in terms of the other:

$$G_{12}(t) = G_{12}(0)e^{-2\int_0^t dt''(\Sigma_1 + \Sigma_2)} - \frac{1}{2}\int_0^t dt' \Sigma_{12} (G_1^{-1} + G_2^{-1}) e^{-2\int_{t'}^t dt''(\Sigma_1 + \Sigma_2)}, \quad (44)$$

which shows that the evolution of the system-environment correlations, and therewith of the whole dynamics, involves characteristic *non-Markovian* features. Furthermore, one may expect a large number of nonzero components in the Fourier spectra of the two-point functions of the system or environment alone. The functions G_{12} , Σ_{12} inherit these and, therefore, the non-Markovian behavior leads to a *quasi stochastic* influence of the environment.

Finally, expanding G_{12} , Σ_{12} for sufficiently short times, we explicitly solve eqs. (41), (43). In the limit of small but finite correlations we obtain:

$$G_{12}(t) \approx G_{12} - 2[(\Sigma_1 + \Sigma_2)G_{12} + \frac{1}{4}(G_1^{-1} + G_2^{-1})\Sigma_{12}]t - \frac{1}{2}\mu^2[G_1^{-1} + G_2^{-1} + O(G_{12}, \Sigma_{12})]t^2, \quad (45)$$

$$\Sigma_{12}(t) \approx \Sigma_{12} + 2[\mu^2 - (\Sigma_1 + \Sigma_2)\Sigma_{12} + \frac{1}{4}(G_1^{-1} + G_2^{-1})G_{12}]t - 2\mu^2[\Sigma_1 + \Sigma_2 + O(G_{12}, \Sigma_{12})]t^2, \quad (46)$$

where all two-point functions on the r.h.s. here assume their initial value ($t = 0$). Note how the analytical behavior changes as $G_{12}(0)$, $\Sigma_{12}(0) \rightarrow 0$.

This is reflected in the decoherence time τ_D of our simple model, which we calculate employing eqs. (34)–(36) of the previous section and assuming small but finite G_{12} , Σ_{12} :

$$\tau_D^{-1} \approx \frac{d}{dt} \ln[G_1 G_2 (G_{12}^2 + \Sigma_{12}^2)]_{t \rightarrow 0} \approx 4(\Sigma_1(0) + \Sigma_2(0)) + \frac{4\mu^2 \Sigma_{12}(0)}{G_{12}(0)^2 + \Sigma_{12}(0)^2}. \quad (47)$$

In the absence of the initial correlations $G_{12}(0)$, $\Sigma_{12}(0)$ the decoherence time vanishes instead, $\tau_D \sim t/2$ ($t \rightarrow 0$). This demonstrates the important role of correlations, which has been investigated in more detail in models of quantum Brownian motion (cf. Section 3), see e.g. Refs.^{12,21}. For an environment without self-interaction at high temperature one finds $\tau_D \propto T^{-1}$.

For the remaining part of this section we neglect the environment, in order to point out an important effect of the TDHF approximation employed in the derivation of the equations of motion (38)–(43). Considering the effective action, eq. (28), it has become obvious that this approximation includes only the $O(\hbar)$ and $O(\hbar^2)$ corrections to the classical action.

Whereas the classical equations of motion of the system alone (1d anharmonic oscillator $\equiv 2$ d.o.f.) can have only regular solutions according to the Poincaré-Bendixson theorem¹³, the potential for *semiquantum chaos* is obvious in the case of the four coupled nonlinear first order equations, cf. eqs. (38)–(40) and (42), representing the system in TDHF. A detailed study of this subset of equations has been made in Ref.²⁰.

Here we represent some illustrating numerical results obtained by integrating the equations of motion forward in time. The initial configuration is a Gaussian wave packet with conserved energy E (all quantities are suitably rescaled and presented in dimensionless form). For the chosen model parameters the minimum of the energy is at $E = -24.3$, the top of the hill separating the two wells of the classical *double-well oscillator* potential is at $E = 0.0$.

In Fig. 4 Poincaré sections for various energies are shown ($\phi \equiv \bar{\Phi}(t)$, $\pi \equiv \bar{\Pi}(t)$). We observe the characteristic break-up of KAM tori as the energy is increased and the corresponding stochastic filling of the ϕ, π phase space¹³. This clearly shows a transition between regular and chaotic motion, which can be associated with tunneling paths, despite the fact that the present classical model is regular²⁰.

Furthermore, in Fig. 5 the behavior the Fourier transform w.r.t. time of a diagonal element of the density matrix is shown. At very low energies (not shown) one finds a simple line spectrum involving the fundamental frequency ω_0 (i.e. harmonic approximation of the potential) or a few multiples thereof (regular motion). At the energies shown the full trajectories are chaotic and produce a broadband noise spectrum. At very high energies the motion becomes regular again with the wave packet experiencing essentially only the anharmonic quartic part of the potential.

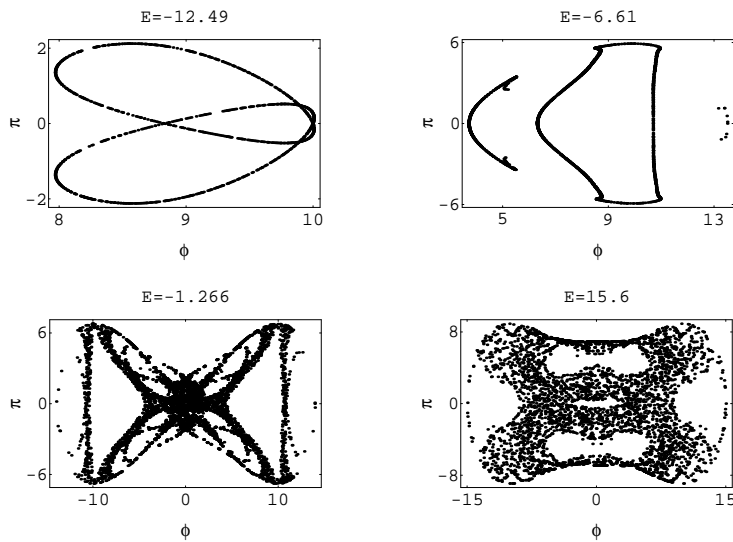


Figure 3: Poincaré sections for the system at various energies (after Ref. [20]) showing the transition to semiquantum chaos, cf. main text.

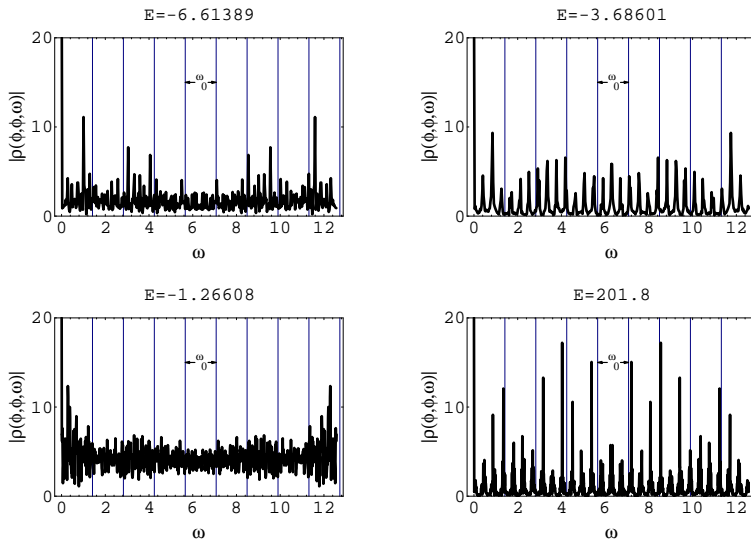


Figure 4: Fourier transform of a diagonal element of the system density matrix at various energies (after Ref. [20]) showing semiquantum chaos as broadband noise in the expected line spectrum (nonlinear resonance at $E=-3.68601$), cf. main text.

These results raise the question of the reliability of the underlying TDHF approximation or analogous semiclassical perturbative expansions around the bare ($\hbar = 0$) classical limit. Generally, the full quantum evolution according to the Schrödinger equation incorporating an environment implies a *linear but non-Markovian master equation* for the system density matrix, which might rule out the possibility of ‘quantum chaos’.

Furthermore, it has recently been shown that *any* variational approximation for a closed system is equivalent to an effective classical Hamiltonian dynamics for the variational parameters²². There, as we have seen in the TDHF case, eqs. (38)–(43), the potential for *semiquantum chaos* arises, if the underlying classical Lagrangian involves higher than quadratic terms. In some examples then, the onset of semiquantum chaos has indeed been related to the breakdown of semiclassical approximations²², even if they do not require weak coupling.

However, the important question remains²⁰, whether there are situations involving (infinitely) many d.o.f., where such approximations could reliably represent the highly complex, even if overall quasi-periodic quantum evolution of the coupled system+environment (fields). Such cases have recently been found in solid state devices. Nevertheless, the real time evolution of fields

which are relevant for high-energy experiments still needs more study, in order to understand decoherence processes, entropy production, and thermalization quantitatively.

5 Conclusions

We have seen in Sections 1, 2 that entropy production in a quantum system can be understood dynamically on the basis of von Neumann's definition of the entropy in terms of its density operator, if and only if the system is coupled to an environment of unobserved or even unobservable degrees of freedom. It induces the necessary quantum decoherence¹.

The example of a nonrelativistic quark in Brownian motion in a simple model of a gluonic environment has been presented (Section 3). It has been pointed out that an environment with a spectral density distribution which is enhanced in the infrared, as compared to the frequently studied 'Ohmic', phonon, or photon environments¹², may lead to interesting squeezing, stabilizing, or enhanced spreading of the wave packet effects, which affect the rate of entropy production.

In order to extend the decoherence approach to field theory, a system and environment consisting of two distinct scalar fields have been studied in the time dependent Hartree-Fock approximation in Section 4⁶. We derived the effective action including up to $O(\hbar^2)$ corrections, the equations of motion, and the entropy functional and discussed their general properties.

Particular attention has been paid to the fact that the approximate semi-classical dynamics may be intrinsically unstable and leading to deterministic semiquantum chaos. It might signal a breakdown of any such approximation scheme for genuinely nonlinear interacting field theories. Whether under these circumstances the initial decoherence, entropy generation, and possibly thermalization in high-energy hadronic or nuclear collisions can be reliably calculated, is an interesting question. The decoherence effects due to initial bremsstrahlung mentioned in Section 2 are presently studied.

Acknowledgements

I thank the members of the Instituto de Física (UFRJ) for their great hospitality and particularly T. Kodama for many stimulating discussions and his support. Discussions with C. E. Aguiar, J. P. Paz, J. Rafelski, S. Rugh and W. Zurek are gratefully acknowledged. This research was supported in part by US-Department of Energy under Grant No. DE-FG03-95ER40937, by NSF under grant INT-9602920, and by Brazil-PRONEX-41.96.0886.00.

References

1. W. H. Zurek, Phys. Today **44**, No. 10, 36 (1991).
2. R. Omnès, Rev. Mod. Phys. **64**, 339 (1992).
3. H. D. Zeh, Phys. Lett. A **172**, 189 (1993).
4. M. Gell-Mann and J. B. Hartle, Phys. Rev. D **47**, 3345 (1993);
in *Complexity, Entropy and the Physics of Information*, ed. W. H. Zurek
(Addison-Wesley, Redwood City, CA., 1990).
5. J. Ellis, N. E. Mavromatos and D. V. Nanopoulos, Mod. Phys. Lett.
A **12**, 1759 (1997); CERN-TH.7000/93 – hep-th/9311148;
Phys. Lett. B **293**, 37 (1992).
6. H.-Th. Elze, Nucl. Phys. B **436**, 213 (1995) (a);
Phys. Lett. B **369**, 295 (1996) (b);
in *Quantum Infrared Physics*, eds. H. M. Fried and B. Müller (World
Scientific, Singapore, 1995) – hep-ph/9407377 (c).
7. P. Braun-Munzinger et al., eds., *Quark Matter '96* (North-Holland, Am-
sterdam, 1996).
8. R. P. Feynman, *Statistical Mechanics* (Benjamin, Reading, Mass., 1974).
9. H.-Th. Elze and U. Heinz, Phys. Rep. **183**, 81 (1989).
10. H.-Th. Elze and P. A. Carruthers, in *Particle Production in Highly Ex-
cited Matter*, eds. H. H. Gutbrod, J. Letessier and J. Rafelski, NATO
ASI series B: Vol. 303 (Plenum, New York, 1994) – hep-ph/9409248.
11. M. Tegmark, Found. Phys. Lett. **6**, 571 (1993).
12. H. Grabert, P. Schramm and G.-L. Ingold, Phys. Rep. **168**, 115 (1988).
13. H. G. Schuster, *Deterministic Chaos*, 2nd ed. (VCH Publishers, Wein-
heim and New York, 1989).
14. W. H. Zurek, S. Habib and J. P. Paz, Phys. Rev. Lett. **70**, 1187 (1993).
15. M. Srednicki, Phys. Rev. Lett. **71**, 666 (1993);
D. Kabat, Nucl. Phys. B **453**, 281 (1995);
E. Benedict and S.-Y. Pi, Ann. Phys. (N.Y.) **245**, 209 (1996).
16. F. Lombardo and F. D. Mazzitelli, Phys. Rev. D **53**, 2001 (1996).
17. R. Jackiw and A. Kerman, Phys. Lett. **71 A**, 158 (1979).
18. J. M. Cornwall, R. Jackiw and E. Tomboulis, Phys. Rev. D **10**, 2428
(1974).
19. J. R. Anglin and W. H. Zurek, Phys. Rev. D **53**, 7327 (1996).
20. Th. C. Blum and H.-Th. Elze, Phys. Rev. E **53**, 3123 (1996).
21. L. D. Romero and J. P. Paz, quant-ph/9612036.
22. F. Cooper, J. Dawson, S. Habib and R. D. Ryne, LA-UR-96-3335 –
quant-ph/9610013.